

The ion energy distribution function in anisotropic plasmas as viewed by charged-exchange based diagnostics in the TJ-Stellarator

J. Arévalo, K. J. McCarthy, J. M. Fontdecaba, B. Van Milligen

Laboratorio Nacional de Fusión, Asociación EURATOM-CIEMAT, 28040 Madrid, Spain

In the TJ-II Stellarator, majority ion temperatures (T_i) obtained by using Neutral Particle Analyzers (NPA) for the toroidal and poloidal directions, usually disagree by a factor of 1.5-2.0 about the plasma magnetic axis (Fig.1). Moreover, Carbon 6+ impurity temperatures (T_C) measured by means of the Charge Exchange Recombination Spectroscopy (ChERS) active technique in the poloidal plane, are higher than poloidal T_i . In this paper, we speculate on an explanation for such observations that is based on the existence of two different dynamics parallel and perpendicular to the local magnetic field and the fundamental differences in the measurement techniques employed.

NPA and ChERS Measurements

For T_i determination [1], cold neutral profiles must be known along the detector's line-of-sight (LOS); if they are not considered, T_i is underestimated. Simulations using flux surface averaged neutral profiles and the measured T_i profile in the poloidal plane[2] show that the offset in poloidal T_i is $\sim 8\%$ for Neutral Beam Injection (NBI) heated plasmas, and $\sim 5\%$ during the Electron Cyclotron Resonance Heating (ECRH) phase. Toroidal temperature correction is less reliable, because the position of toroidal NPA is fixed ($\rho \sim 0.2$), and so, no profiles are available. Assuming a similar T_i profile for both views, an offset of 10-6% is found in the toroidal NPA T_i . Therefore, although toroidal LOS has a complicate path along the plasma, Fig. 2, the offset in T_i measurements is similar for both views. However, we do not rule out a sharper toroidal T_i profile, and therefore, a higher offset

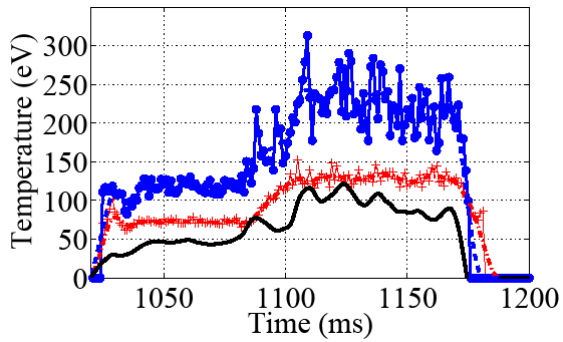


Figure 1. Toroidal (blue), poloidal (red) and the difference between both temperatures (black).

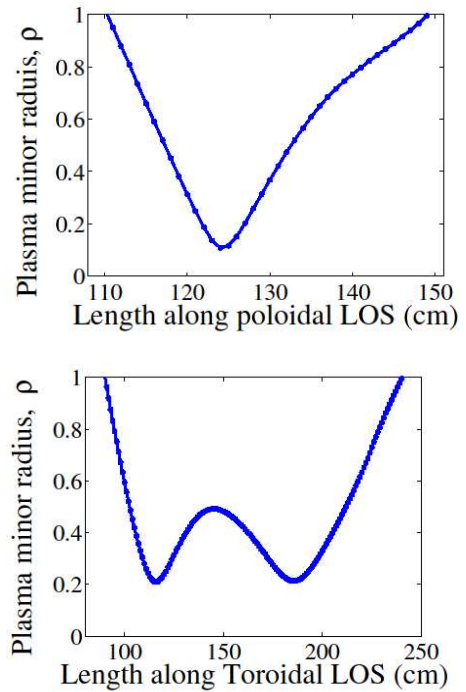


Figure 2. Variation of ρ along poloidal and toroidal LOS.

on main ion toroidal temperature.

C^{6+} impurity temperatures [3] greatly exceeds T_i (see Fig. 1 and 3) although for TJ-II conditions both species should be in thermal equilibrium. A source of error could be the energy tails due to suprathermal populations [4]. In the toroidal NPA's energy spectrum, a hotter tail is observed for energies quite above 1 keV, but T_i calculations are performed in the 0.2-1 keV interval. Hence, suprathermal populations do not contaminate NPA measurements. However, these tails could have a great impact in ChERS temperature measurements during ECRH phase. Therefore, a comparison between T_i and T_C during ECRH phase will not be presented here.

EDF viewed by a diagnostic

NPA's measurements suggest that two different temperatures in the parallel and perpendicular directions to the local magnetic field exist simultaneously. Thus, an anisotropic energy distribution function (EDF) should be used. To estimate how this EDF is viewed in an external reference system -given by a diagnostic-, the magnetic frame is rotated towards the diagnostic reference system. The transformation must be invariant against rotation around \vec{B} (because of the cyclotron symmetry), but also against rotation around the LOS direction of the detector (let us say U), because there is no privileged direction in its perpendicular plane. Hence, the axes can be chosen so only a rotation of angle α is needed:

$$f(v_u, v_{u\perp 1}, v_{u\perp 2}) = \frac{n}{(2\pi)^{3/2} v_{th,\parallel} v_{th,\perp}^2} \exp\left(-\frac{av_u^2}{2} - \frac{v_{u\perp 1}^2}{2v_{th,\perp}^2} - \frac{bv_{u\perp 2}^2}{2} + cv_u v_{u\perp 2}\right) \quad (1.1)$$

$$a = M \frac{T_\perp \cos^2 \alpha + T_\parallel \sin^2 \alpha}{T_\parallel T_\perp} \quad b = M \frac{T_\perp \sin^2 \alpha + T_\parallel \cos^2 \alpha}{T_\parallel T_\perp} \quad c = M \sin \alpha \cos \alpha \frac{T_\perp - T_\parallel}{T_\parallel T_\perp}$$

This formula stands for a diagnostic view, U , defined in a direction of angle α with the magnetic field (such as $\cos \alpha = \hat{u}_U \cdot \hat{b}$). The directions $v_{u\perp 1}$ and $v_{u\perp 2}$ are arbitrary, and do not appear in the final expression of the EDF.

For neutral particle measurements, there is a restriction over the detected velocities [5]: only those particles which escape from the plasma within the solid angle of the detector will be measured. In the TJ-II, NPA's solid angle is really small, about $\Omega \sim 10^{-8} \text{ str}$; as a result, the EDF viewed by this diagnostic will not detect the whole velocity distribution. The local temperature observed by a NPA is:

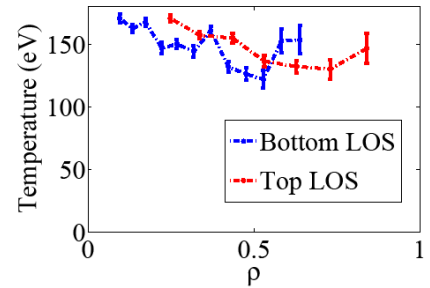


Figure 3. Poloidal C VI temperature measured by CXRS with two opposing views (i.e., bottom and top)

$$T_{NPA}(U) := \frac{T_{\parallel}T_{\perp}}{T_{\perp} \cos^2 \alpha + T_{\parallel} \sin^2 \alpha} \quad (1.2)$$

In the case of Doppler-based measurements, there is no restriction over particle velocities, but over the direction of the emitted photon (through its wave-number unit vector, \hat{k}). Thus, as Doppler broadening, and hence photon wavelength, are related to impurity thermal velocities, ChERS does not eliminate any velocity component: $v_u = \vec{v} \cdot \vec{dl} = c\Delta\lambda / \lambda_0 \quad \forall v_{u\perp 1}, v_{u\perp 2}$. Therefore, we must integrate these components over $(-\infty, \infty)$ in eq. (1.1). The temperature observed by the ChERS diagnostic results,

$$T_{CXRS}(U) := T_{\perp} \sin^2 \alpha + T_{\parallel} \cos^2 \alpha \quad (1.3)$$

The temperatures defined by eq. (1.2) and (1.3) vary with the local magnetic field, but also with the position of each diagnostic. It must be noted that these are local values.

Reconstruction

In the TJ-II there are five independent measurements of the temperature: two poloidal plus one toroidal obtained through neutral analysers; and two poloidally located ChERS observations. In order to check out this model, we can estimate the temperature which should see the toroidal NPA at $\rho \sim 0.2$, from the data measured by poloidal NPA and ChERS:

$$T_{\perp} = \frac{T_1 - \sqrt{T_1^2 - 4T_{CXRS}T_{NPA} \sin^4(\alpha)}}{2 \sin^2(\alpha)} \quad T_{\parallel} = \frac{T_{CXRS} - T_{\perp} \sin^2(\alpha)}{\cos^2(\alpha)} \quad (1.4)$$

Here, $T_1 = T_{CXRS} - T_{NPA} \cos(2\alpha)$. Poloidal NPA and ChERS are located in almost the same toroidal angle, and so $\alpha \approx 62^\circ$ for both of them. The measured T_c , in the time of injection of the Diagnostic Neutral Beam ($t_{DNBI} = 1150$ ms), was ~ 170 eV, Fig. 3. At the same time, $T_{NPA-Pol} \sim 135$ eV (after taking into account the $\sim 8\%$ offset). Substituting these values in (1.4) it is obtained: $T_{\perp} = 115$ eV and $T_{\parallel} = 366$ eV. The local toroidal temperature measured by the NPA will be (eq. (1.2), $\alpha \approx 28, 1^\circ$) $T_{NPA-Tor} = 247$ eV. After applying the simulated $\sim 10\%$ offset for toroidal T_i in NBI plasmas, $T_{NPA-Tor} \sim 224$ eV. This value agrees with the experimental 209eV, with a 7% of error (see Fig. 1). Nevertheless, this 10% offset has been obtained after using a shape similar to the flat profiles measured by the poloidal NPA. There is no *a priori* reason to admit this statement, for poloidal T_i is mainly determined by T_{\perp} , and toroidal T_i by T_{\parallel} . Just by taking a $\sim 15\%$ offset, the experimental value is retrieved.

Finally, time evolution of T_{\parallel} and T_{\perp} can be obtained from the local poloidal and toroidal NPA

temperatures *i.e.*, after correcting for the offset due to line averaged measurements-. This evolution is shown in Fig. 4. It is observed how, whereas the initial differences between toroidal and poloidal T_i were ~ 50 eV during ECRH phase, and 100 eV during the NBH phase, the difference between T_{\parallel} and T_{\perp} has been doubled. Further studies are needed to understand why the ratio T_{\parallel}/T_{\perp} increases during NBI phase: this is not intuitive, because the higher collisionality during this regime should reduce the anisotropy. The higher value of T_{\parallel} could be related with TJ-II magnetic topology and so, with magnetic trapping.

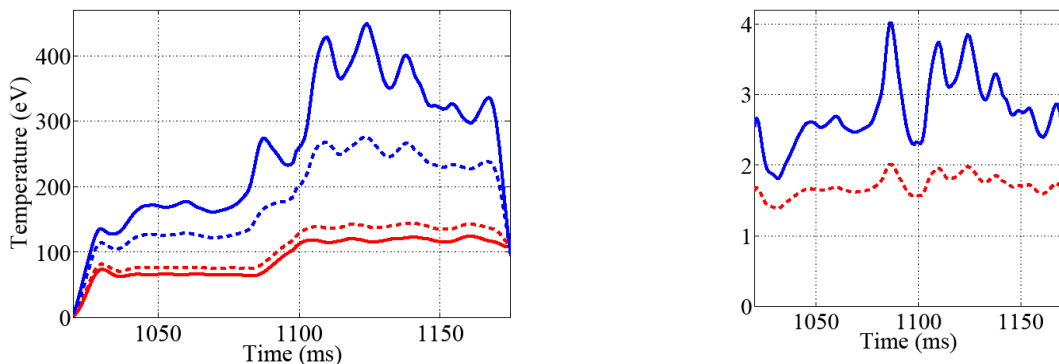


Figure 4. (Left) Reconstruction of time evolution of T_{\parallel} (solid blue line) and T_{\perp} (solid red line) from T_i measured by toroidal NPA (dashed blue line) and poloidal NPA (dashed red line). (Right) Ratio T_{\parallel}/T_{\perp} (blue) and $T_{NPA-Tor}/T_{NPA-Pol}$ (red).

Conclusions

Local velocity and energy distribution functions are proposed for ChERS and NPA diagnostics, when a T_{\parallel} different from T_{\perp} exists in a plasma. The directionality of NPA measurements prevents some velocities from being detected; in contrast, ChERS diagnostic weight each Doppler shifted velocity, v_u , with all the velocities in the orthogonal velocity plane. As a consequence, the disagreement between T_C and T_i measurements is explained, for NBI heated plasmas. Besides, time evolution of T_{\parallel} and T_{\perp} has been obtained from toroidal and poloidal NPA temperatures, showing that the energy stored in the parallel dynamics not only exceeds the perpendicular one, but is much greater than the measured toroidal T_i .

References

- [1] F Wagner, J.Vac.Sci.Technol. 20, 1211 (1982)
- [2] J M Fontdecaba et al., Plasma and Fusion Research
- [3] J Arévalo et al., 18th Topical Conf. on High Temperature Plasma Diagnostics, New Jersey 2010.
- [4] D. Rapisarda et al., Plasma Phys. Contol. Fusion 49, 309 (2007).
- [5] K G McClements et al., Nuclear Fusion 37, 473 (1999)